ACS Energy LETTERS

http://pubs.acs.org/journal/aelccp

Glycerol Oxidation Pairs with Carbon Monoxide Reduction for Low-Voltage Generation of C_2 and C_3 Product Streams

Hossein Yadegari, Adnan Ozden, Tartela Alkayyali, Vikram Soni, Arnaud Thevenon, Alonso Rosas-Hernández, Theodor Agapie, Jonas C. Peters, Edward H. Sargent, and David Sinton*

Cite This: *ACS Energy Lett.* 2021, 6, 3538−3544

Read Online

ACCESS | Metrics & More | Article Recommendations | Supporting Information

ABSTRACT: **Electrochemical carbon dioxide reduction to multicarbon products provides the storage of renewable energy in the form of chemical bonds, as well as a means to displace fossil sources of chemical feedstocks. However, the accompanying anodic oxygen evolution reaction (OER) reduces the energy efficiency of the process without providing a salable product. Replacing OER with alternative organic oxidation reactions (OORs) is an emerging strategy to reduce the full-cell potential and generate valuable products on both sides of the cell. We pursue carbon monoxide reduction that avoids carbonate formation and benefits from highly alkaline anode conditions favorable for OOR. This coelectrolysis strategy achieves a cathodic C_{2+} product stream (71% FE) and an anodic C_3 product stream (75% FE) at 180 mA cm^{-2} with a full-cell potential of 1.34 V. The integrated system reduces the CO-to-C_2H_4 energy requirement by 55% (to ~72 GJ/ton_C_2H_4), halving the projected energy cost of ethylene production from CO_2.**

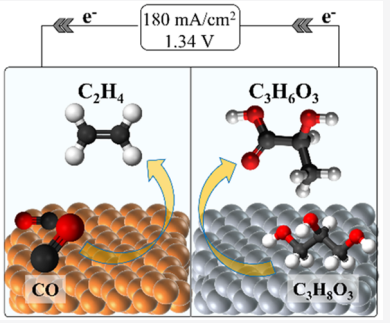

Decarbonization of energy generation and chemical production motivates the conversion of renewably generated electrical energy into commodity fuels and chemicals. Electrocatalytic conversion of CO_2 to chemicals provides a means to store intermittent renewable energy and displace fossil-fuel-based chemical production.[1]

With a global annual production of 192 Mt in 2019,[2] ethylene (C_2H_4) is the most in-demand multicarbon product accessible via the CO_2 reduction reaction (CO_2RR). C_2H_4 is currently produced through energy-intensive steam cracking of long-chain hydrocarbons which produce 2−3 tCO_2/tC_2H_4.[3] CO_2 electrolyzers can produce C_2H_4 with high Faradaic efficiencies (FEs) of 70−80% and energy efficiencies (EEs) over 30% at current densities greater than 100 mA cm^{-2}.[4−7] However, this process does not currently compete with the incumbent thermochemical route in production costs and energy input.[8] The conversion of CO_2 to C_2H_4 requires an electrical energy input of 196 GJ/tC_2H_4 (at today's best with 80% FE, 30% EE), and this corresponds to $1340/$tC_2H_4$ in electricity cost alone (at $0.03/kWh). These values greatly exceed the energy value of C_2H_4 at 49.4 GJ/tC_2H_4 and therefore also its market price of ~$800/$tC_2H_4$. Addressing these limitations will require innovation on both sides of the cell.

Present-day CO_2 electrolyzers employ the oxygen evolution reaction (OER) as the counter anodic half-reaction. On the basis of Gibbs free energy, up to 90% of input energy is consumed by OER in an idealized CO_2 electrolyzer.[8] Our empirical analysis of voltage distribution in a membrane electrode assembly (MEA) electrolyzer indicated that sluggish OER kinetics accounts for 50% of the imposed overpotential to the cell.[9] The value of the produced oxygen (~$25/$tO_2$) is negligible and does not contribute to economic feasibility. Replacing OER with organic oxidation reactions (OORs) is an emerging strategy to lower the full-cell potential in CO_2 electrolyzers[10−15] as well as electrochemical hydrogen generation[16−18] and to produce valuable anodic products.[19−21]

Electrooxidation of organic biomass conforms with the principal process design rules of low feed cost, high product market price, and a market size suitable to be paired with CO_2RR.[8,19] Glycerol is a low-cost byproduct of surfactant and biodiesel production from vegetable oils and waste fats[22,23] and has been emphasized as a promising anode-side reactant[8] for CO_2RR that could reduce the full-cell potential and provide value-added products. Lactic acid (or lactate in the conjugate base form) is a product of particular interest for the production

Received: August 4, 2021

https://doi.org/10.1021/acsenergylett.1c01639
ACS Energy Lett. 2021, 6, 3538−3544

Scheme 1. CORR-OOR versus CORR-OER[a]

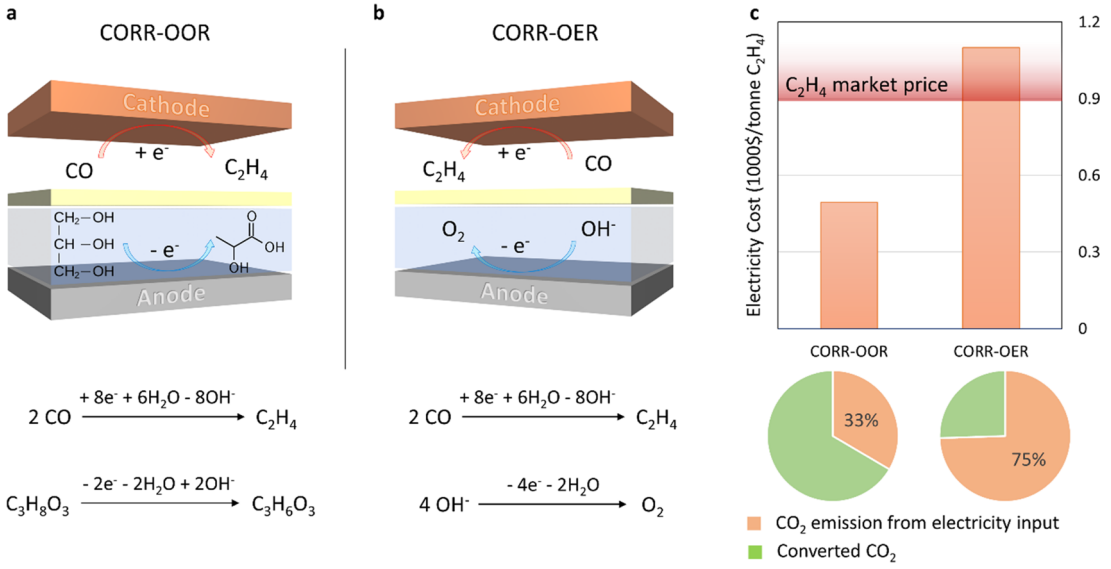

[a]Schematic MEA diagrams for CORR-OOR (a) and CORR-OER (b) systems along with cathodic and anodic electrochemical reactions; (c) comparison of the electricity costs as well as CO_2 emissions associated with electricity generation calculated based on the performance metrics obtained for both systems. The grid emission factor (GEF) was considered to be 0.51 kg CO_2/kWh.

of biodegradable thermoplastic, poly(lactic acid), which accounts for 10% of current bioplastics.[24] To realize the benefits of coelectrolysis of anode and cathode products, the reactions must be compatible within a single system—electrolyte, membrane, and temperature—at practical reaction rates (>100 mA cm^{-2}).[25] To date anodic upgrading of glycerol has been limited to <10 mA cm^{-2}.[21,26]

Here we find OOR to be incompatible with carbon dioxide reduction to ethylene in an MEA. On the cathode, hydrogen evolution dominates because of the loss of CO_2 reactant to carbonate. On the anode, OOR fails to compete with oxygen evolution beyond a moderate reaction rate because of the relative abundance of water. We pursue carbon monoxide reduction that benefits from highly alkaline anodic conditions and avoids CO_2 reactant loss to carbonate and associated losses.[27−29] This approach motivates a two-step cascade with CO_2 to CO via established solid oxide technology, followed by CO to higher value products.[30] The second step can also facilitate organic oxidation reactions such as glucose oxidation.[30] We develop the coelectrolysis of CO and glycerol here to reduce the energy required for C_2 cathode products while producing a second stream of valuable C_3 products with large market size. To overcome the kinetic limitations to high-rate OOR, we develop a hierarchical hydrophilic nanostructured catalyst that accelerates the transfer of charge and hydrophilic organic reactants. As a result, we achieve high-rate coproduction of valuable C_2 and C_3 product streams at a low full-cell voltage of 1.34 V at 180 mA cm^{-2}.[31]

Optimization of reaction parameters in a three-electrode cell indicated that OOR delivers highest current densities using Pt/C electrode in high alkaline solution (see Supplementary Notes 1 and 2).[26] We then paired CO_2RR with the optimized OOR by feeding glycerol in 2.0 M KOH electrolyte into a standard CO_2RR MEA electrolyzer.[9] All the electrocatalytic measurements were performed using gas diffusion layer (GDL) electrodes. Copper-coated GDL was used as the cathode separated by an anion exchange membrane (AEM) from Pt/C-coated GDL anode (see the Supporting Information for details). Analysis of the cathodic gas products in the current density range of 20 to 300 mA cm^{-2} (Figure S6) indicated hydrogen (H_2) to be the major product, with C_2H_4 FE not exceeding 15%. The dominance of HER at these alkaline conditions indicated a low CO_2 concentration at the catalyst surface—an artifact of severe CO_2 reactant loss to carbonate that is typical at high alkalinity in these systems.[27,32] In addition, the rapid increase in the full-cell potential when current density increased from 60 to 120 mA cm^{-2} suggests a transition from the desired OOR back to high thermodynamic-potential OER. The control case of CO_2RR-OER exhibited a similar C_2H_4 content with slightly higher CO/H_2 ratio (Figure S7).

Decreasing the anolyte KOH concentration 20-fold (0.1 M KOH) suppressed hydrogen evolution in favor of CO production, without a significant improvement in C_2H_4 activity (Figure S8). However, the full-cell potential increased because of the higher anodic potentials. A similar product distribution was achieved in the control, CO_2RR-OER experiment with 0.1 M KOH anolyte (Figure S9). These results indicate the incompatibility of CO_2RR and alkaline OOR. The high anolyte pH required for OOR on the anode side results in extreme CO_2 reactant loss and low C_2 selectivity on the cathode side. Although high C_2 selectivity can be achieved in a flow-cell configuration under alkaline conditions,[4,7] the loss of reactant CO_2 to carbonates results in unacceptably high operation costs.[27] We conclude that the promise of glycerol oxidation cannot be realized in conventional CO_2RR systems.

Carbon monoxide reduction exhibits high C_2 product efficiency under highly alkaline conditions,[30,33] offering compatibility with glycerol oxidation. Moreover, electrochemical conversion of the CO_2-to-CO step is maturing rapidly, with efficiencies greater than 90% now achieved at industrial scale.[29,34] The effectiveness of the CORR step is now limiting on the path of CO_2 conversion to multicarbon products.

Both OOR and OER configurations were tested in an MEA electrolyzer (Scheme 1a,b). CO was fed onto a similar copper-

https://doi.org/10.1021/acsenergylett.1c01639
ACS Energy Lett. 2021, 6, 3538−3544

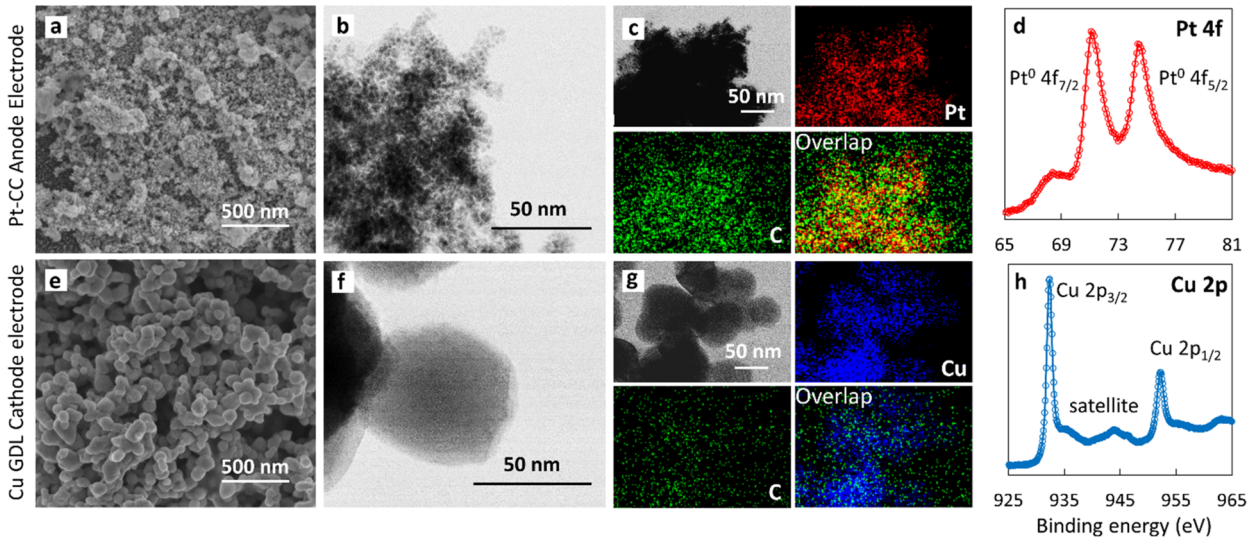

Figure 1. Characterization of the synthesized anode (OOR) and cathode (CORR) electrodes. (a and e) Scanning electron microscopy (SEM) and (b and f) transmission electron microscopy (TEM) micrographs of Pt-CC and Cu GDL electrodes. (c and g) Energy-dispersive X-ray (EDX) elemental maps for Pt-CC and Cu GDL electrodes. (d and h) X-ray photoelectron spectroscopy (XPS) results for Pt-CC and Cu GDL electrodes.

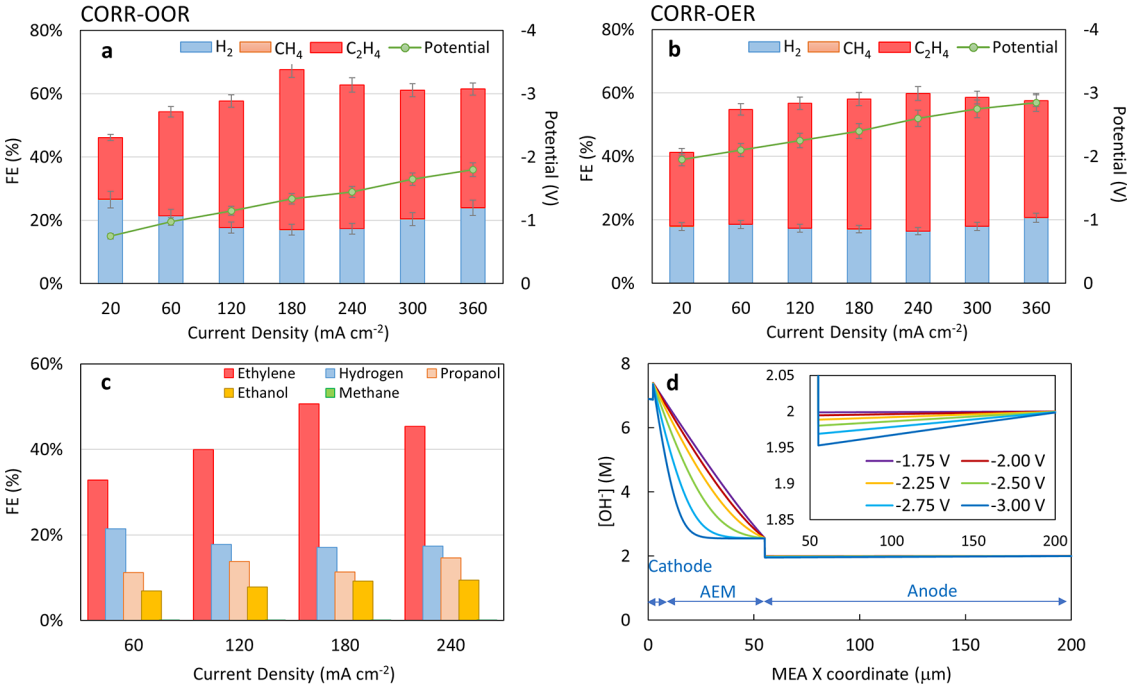

Figure 2. Electrochemical performance of the CORR-OOR system compared with the conventional OER counterpart. (a and b) Selectivity of the gaseous cathodic products for CORR-OOR (a) and CORR-OER (b) systems. (c) Selectivity of the cathodic products for CORR-OOR system at different current densities. The anolyte was 2.0 M KOH + 4.0 M glycerol solution in the case of CORR-OOR and 2.0 M KOH in the case of CORR-OER. (d) Simulation of OH^- concentration throughout MEA cell using COMSOL for CORR-OOR system.

coated GDL separated from the anode by an AEM. Glycerol was dissolved in the anolyte. The CORR-OOR cell provided 51% FE for C_2H_4 at 1.34 V (180 mA cm^2). The control case of CORR-OER provided 41% FE for C_2H_4 at 2.40 V (180 mA cm^2). We estimated the electrical energy input for production of one tonne of C_2H_4 by both approaches using the full cell voltages and Faradaic efficiency values obtained here through eqs 9−11 (Supporting Information). We found that C_2H_4 produced in the CORR-OER process would not be profitable based on the cost of input electricity alone (Scheme 1c). In addition, emissions associated with the electrical energy input would be 75% of the converted CO_2, based on the current grid emission factor (GEF).[8] With reduced energy demand, the grid electricity emissions are reduced to 33% of converted CO_2 in the CORR-OOR case.

We explored C_2H_4 production in the CORR-OOR pair as a function of glycerol and KOH concentrations using a Pt/C catalyst loaded GDL. Figure S10 and S11 compare the gas product distribution at different glycerol and KOH concentrations, respectively. The partial current density of C_2H_4

https://doi.org/10.1021/acsenergylett.1c01639
ACS Energy Lett. 2021, 6, 3538−3544

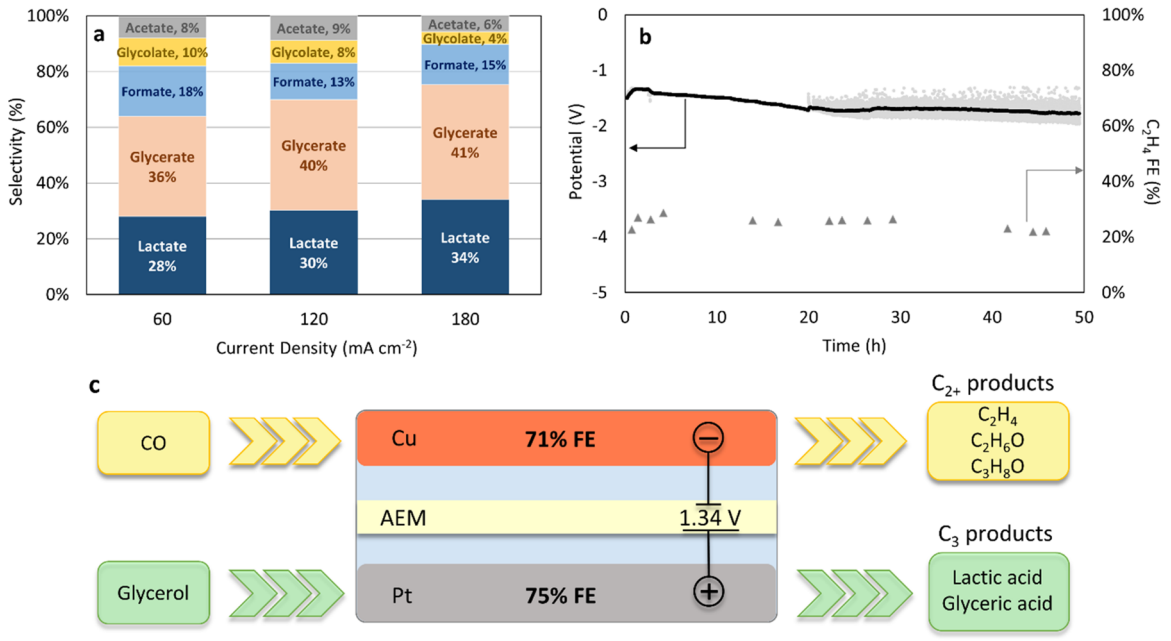

Figure 3. Analysis of the anodic products and long-term stability of CORR-OOR system. (a) Selectivity of anodic products at different current densities in CORR-OER system using Pt-CC electrode. The anolyte was 4.0 M glycerol in 2.0 M KOH solution. (b) Extended CORR-OOR performance at 100 mA cm^{-2} using 4.0 M glycerol in 2.0 M KOH as anolyte. (c) Schematic of the CORR-OOR system inputs and outputs for simultaneous production of C_2 and C_3 streams.

normalized by cell potential ($J_{C_2H_4}$/potential) at fixed current (120 mA cm^{-2}) provided a means of assessing performance as a function of KOH and glycerol concentrations (Figure S12). The system provided the highest C_2H_4 partial current density (37 mA cm^{-2}) at a low full-cell potential (1.25 V), with 4.0 M glycerol in 2.0 M KOH anolyte. However, practical application of COR-OOR will require still higher reaction rates.[1]

We sought to accelerate anode reaction kinetics by reducing mass and charge transfer resistances. With glycerol being hydrophilic, we envisioned an ideal OOR electrode to provide a hierarchical hydrophilic framework exposing the high surface area of active catalyst. A hydrophilic carbon cloth (CC) provided a three-dimensional substrate, and Pt catalyst was synthesized directly on the carbon cloth (see the Supporting Information for details). The synthesized Pt-CC electrode provides a dual-porous network comprising the CC substrate decorated with Pt nanoparticles smaller than 5 nm (Figures 1a and S13). While hydrophobic Pt/C-loaded GDL showed a sharp jump in full cell potential at 180 mA cm^{-2} (Figure S10c), the Pt-CC electrode maintained a low potential up to 360 mA cm^{-2}. Considering the similar loading of Pt on both electrodes, the improved electrochemical performance is attributed to enhanced mass transport in the Pt-CC case. The hydrophilic macropores in the CC substrate enable mass transport through the electrode while the small Pt nanoparticles expose a large area of catalytic active sites with which to achieve high current density.

Transmission electron microscopy (TEM) analysis of the Pt-CC electrode indicates aggregates of nanoparticles smaller than 5 nm (Figures 1b and S14). Moreover, energy dispersive X-ray (EDX) mapping of the sample shows a uniform mixture of Pt and carbon (Figure 1c). A similar microporous structure was prepared for the cathode electrode by coating Cu nanoparticles (25 nm) on a hydrophobic GDL. Spherical Cu nanoparticles smaller than 50 nm can be seen in the TEM micrographs (Figure 1e,f) as well as EDX mapping (Figure 1g). TEM images shown in Figure S15 further confirm the uniform dispersion of ionomer on Cu nanoparticles. Ex situ X-ray photoelectron spectroscopy (XPS) indicates the presence of metallic Pt and Cu, at anode and cathode, respectively (Figure 1d,h).

Using the hierarchical hydrophilic anode, the CORR-OOR system could achieve current densities up to 360 mA cm^{-2} without transitioning to OER. The attained OOR current density on the synthesized anode is 3-fold higher than that of a commercial Pt/C electrode (also see Figure S10). The highest C_2H_4 FE (51%) was achieved at 180 mA cm^{-2} for CORR-ORR—a notable increase compared with the CORR-OER control case C_2H_4 FE (41%) (Figure 2a,b). The increased C_2H_4 FE is attributed to the enhanced kinetics of OOR compared to OER, with the OOR anode providing rapid OH^- consumption and thereby accelerating the transport of OH^- from the cathode. Ethanol and propanol were also detected, accounting for ~20% of the cathodic FE (Figure 2c). The remaining FEs are attributed to formate and acetate that migrated to the anode side (formate and acetate were detected in excess of these levels in the anolyte; the cumulative composition is reported in the anodic stream).

The full-cell potentials of CORR coupled with OER and OOR are compared in Figure S16. The CORR-OOR system realized over 1.0 V reduction in full-cell potential compared with CORR-OER, over the whole current density range, corresponding to a 47% reduction in cell voltage. The reduced full-cell potential decreases the required energy input for C_2H_4 synthesis from 161 GJ/tC_2H_4 in CORR-OER (Supporting Information) to 72 GJ/tC_2H_4 in the CORR-OOR process. As the most energy-intensive step in the tandem process,[29,30] this improvement in CORR corresponds to a net energy input reduction approaching 50% for the full CO_2-to-C_2H_4 cascade.

To further assess the effect of OOR kinetics on the cell performance, we modeled the system as a one-dimensional

https://doi.org/10.1021/acsenergylett.1c01639
ACS Energy Lett. 2021, 6, 3538−3544

MEA (see Supporting Information for details). The simulations predict hydroxyl ion (OH^-) concentration through the MEA under different applied potentials for OOR and OER (Figures 2d and S17). The concentration of OH^- at the anode decreases with increasing cell potential for both OOR and OER. However, the enhanced kinetics of OOR results in a faster consumption of OH^- and a lower OH^- concentration at the anode side (inset of Figure 2d). The OOR anode accelerates OH^- transfer through the MEA, benefiting both sides of the cell. In addition, the OH^- concentration profile in the AEM changes from linear to highly nonlinear with increasing cell potential.[35] This transition is explained by the increased production of OH^- ions at the cathode along with faster consumption of OH^- ions at the anode. The mass transport of OH^- ions through the MEA limits the C_2H_4 partial current density, resulting in reduced C_2H_4 FE at current densities greater than 180 mA cm^{-2}.

The anode side OOR products were analyzed using proton nuclear magnetic resonance (^1H NMR) spectroscopy (Figure 3a). The CORR-OOR system exhibited a stable conversion efficiency during 50 h of continuous operation at 100 mA cm^{-2} (Figure 3b). Oxidation of glycerol on the Pt-CC electrode resulted in formation of more than 70% C_3 products at 120 and 180 mA cm^{-2} with lactate (30−34%) and glycerate (40−41%) as the major products. Glycolate, acetate, and formate were also detected as C−C cleavage products at lower concentrations. Each product is an upgrade from glycerol input, with individual values ranging from 3- to 8-fold that of the glycerol input (Table S2). Glycerate has industrial application in poly(glyceric acid carbonate) production, which is a degradable analogue of poly(acrylic acid) with annual demand on the multimillion ton scale.[36] Lactic acid (lactate in the conjugate base form) is the most viable product, with a high value (1.58−1.87 $/t). It is used widely in the food industry and in bioplastic production with an annual market size of millions of tonnes.[37]

To steer the OOR reaction to lactate, we explored further the oxidation of glycerol on Pt at alkaline conditions. The reaction is known to proceed through the oxidation of the primary alcohol groups to produce glyceraldehyde.[38] Further oxidation of glyceraldehyde on the Pt surface results in formation of glycerate which in turn produces glycolate and formate through C−C cleavage (path I in Figure S18).[38] At alkaline conditions, glyceraldehyde may also undergo base-catalyzed dehydration followed by intermolecular Cannizzaro rearrangement to produce lactate.[26] However, further oxidation of lactate to lower-valued acetate and formate through C−C cleavage is a risk (path II in Figure S18). As Pt also catalyzes the C−C cleavage reaction that results in increasing the undesirable C_2/C_1 products in anodic stream, we considered partial replacement of Pt with Pd—an approach that has been shown to reduce C−C bond cleavage in glycerol oxidation.[26,39] We synthesized and tested a Pt/Pd-CC (50 wt % Pd) electrode. However, the partial replacement of Pt with Pd slightly decreased the C_2H_4 FE at the cathode and increased the full-cell potential because of the lower oxidation activity of Pd, resulting in a transition from OOR to OER between 60 and 120 mA cm^{-2} (Figure S19). Moreover, analysis of the anode stream products indicated increased formate production (Figure S20). This result highlighted the importance of Pt electrode activity in achieving high current densities for OOR in the paired electrolyzer. In contrast with the conventional electrochemical cells,[26] the glycerol oxidation in the paired flow-cell electrolyzer is a function of whole-cell kinetics, local pH conditions, and mass transfer.

The paired CORR-OOR system (Figure 3c) decreased the required energy for the CO-to-C_2H_4 process to ∼72 GJ (ton $C_2H_4)^{-1}$, which corresponds to 55% in energy saving compared with the conventional CORR-OER (∼161 GJ (ton $C_2H_4)^{-1}$). The reduced energy input results in lowering the electricity cost below the C_2H_4 market price (∼$494 (ton $C_2H_4)^{-1}$ for CORR-OOR versus ∼$1100 (ton $C_2H_4)^{-1}$ for CORR-OER) to achieve profitable ethylene electroproduction. In addition, the value-added C_3 stream produced in the anode side increases the profitability of the electrolyzer as a system.

The developed CORR-OOR in this study offers a viable alternative for electrochemical synthesis of C_2H_4 that advances both economical profitability and carbon neutrality. CORR eliminated CO_2 loss to carbonate formation which consumes the majority of energy input in CO_2 electroreduction. Pairing CORR with glycerol oxidation using an alkaline anolyte enabled a synergistic effect between cathodic and anodic reactions, producing C_{2+} products with more than 71% FE at the cathode. A hierarchical anode structure with nanoporous catalytic reaction sites enabled C_3 products with 75% selectivity at the anode under industrially relevant current density of 180 mA cm^{-2}. Replacing sluggish OER with glycerol oxidation reduced the full-cell potential by over 1 V, with an associated 49% reduction in energy required for the overall CO_2-to-CO and CO-to-C_2H_4 process. The increasing global biofuel production is expected to provide a steady supply of low-cost glycerol while the growing demand for biodegradable polymers expands the market for renewably generated lactic acid. More generally, the dual C_2 and C_3 product outputs demonstrated here provide a model for paired reactions and a whole-cell approach to the efficient electroproduction of chemicals.

■ ASSOCIATED CONTENT

Supporting Information

The Supporting Information is available free of charge at https://pubs.acs.org/doi/10.1021/acsenergylett.1c01639.

Experimental data, electrochemical and microscopy data, SEM micrographs, gas and liquid analysis results, and Faradaic efficiency calculations (PDF)

■ AUTHOR INFORMATION

Corresponding Author

David Sinton − *Department of Mechanical and Industrial Engineering, University of Toronto, Toronto, Ontario M5S 3G8, Canada;* orcid.org/0000-0003-2714-6408; Email: sinton@mie.utoronto.ca

Authors

Hossein Yadegari − *Department of Mechanical and Industrial Engineering, University of Toronto, Toronto, Ontario M5S 3G8, Canada;* orcid.org/0000-0002-2572-182X

Adnan Ozden − *Department of Mechanical and Industrial Engineering, University of Toronto, Toronto, Ontario M5S 3G8, Canada*

Tartela Alkayyali − *Department of Mechanical and Industrial Engineering, University of Toronto, Toronto, Ontario M5S 3G8, Canada;* orcid.org/0000-0003-3895-8700

https://doi.org/10.1021/acsenergylett.1c01639
ACS Energy Lett. 2021, 6, 3538−3544

Vikram Soni − *Department of Mechanical and Industrial Engineering, University of Toronto, Toronto, Ontario M5S 3G8, Canada;* orcid.org/0000-0001-9354-475X
Arnaud Thevenon − *Joint Center for Artificial Photosynthesis and Division of Chemistry and Chemical Engineering, California Institute of Technology, Pasadena, California 91125, United States;* orcid.org/0000-0002-5543-6595
Alonso Rosas-Hernández − *Joint Center for Artificial Photosynthesis and Division of Chemistry and Chemical Engineering, California Institute of Technology, Pasadena, California 91125, United States;* orcid.org/0000-0002-0812-5591
Theodor Agapie − *Joint Center for Artificial Photosynthesis and Division of Chemistry and Chemical Engineering, California Institute of Technology, Pasadena, California 91125, United States;* orcid.org/0000-0002-9692-7614
Jonas C. Peters − *Joint Center for Artificial Photosynthesis and Division of Chemistry and Chemical Engineering, California Institute of Technology, Pasadena, California 91125, United States*
Edward H. Sargent − *Department of Electrical and Computer Engineering, University of Toronto, Toronto, Ontario M5S 3G4, Canada;* orcid.org/0000-0003-0396-6495

Complete contact information is available at: https://pubs.acs.org/10.1021/acsenergylett.1c01639

Author Contributions

D.S. and E.S. supervised the project. H.Y., D.S., and A.O. conceived the idea and designed the experiments. H.Y. carried out the experiments, collected and analyzed the data, and wrote the manuscript. A.O. aided with electrochemical measurements and analytical characterizations. T.A. performed the COMSOL modeling. All authors discussed the results and contributed to manuscript editing.

Notes

The authors declare no competing financial interest.

■ ACKNOWLEDGMENTS

The authors acknowledge Ontario Centre for the Characterization of Advanced Materials (OCCAM) for sample preparation and characterization facilities. The authors acknowledge financial support from the Ontario Research Foundation: Research Excellence Program; the Natural Sciences and Engineering Research Council (NSERC) of Canada; the CIFAR Bio-Inspired Solar Energy program; and the Joint Centre of Artificial Synthesis, a DOE Energy Innovation Hub, supported through the Office of Science of the US Department of Energy under Award No. DE-SC0004993. D.S. acknowledges the NSERC E.W.R Steacie Memorial Fellowship. A.T. acknowledges Marie Skłodowska-Curie Fellowship H2020-MSCA-IF-2017 (793471). Infrastructure support from the Canada Foundation for Innovation and the Ontario Research Fund are also gratefully acknowledged.

■ REFERENCES

(1) De Luna, P.; Hahn, C.; Higgins, D.; Jaffer, S. A.; Jaramillo, T. F.; Sargent, E. H. What would it take for renewably powered electrosynthesis to displace petrochemical processes? *Science* **2019**, *364* (6438), eaav3506.
(2) Global Ethylene Industry Outlook to 2024 - Capacity and Capital Expenditure Forecasts with Details of All Active and Planned Plants. https://store.globaldata.com/report/gdch0090icr--global-ethylene-industry-outlook-to-2024-capacity-and-capital-expenditure-forecasts-with-details-of-all-active-and-planned-plants/.
(3) Ren, T.; Patel, M.; Blok, K. Steam cracking and methane to olefins: Energy use, CO2 emissions and production costs. *Energy* **2008**, *33*, 817−833.
(4) Dinh, C. T.; Burdyny, T.; Kibria, M. G.; Seifitokaldani, A.; Gabardo, C. M.; de Arquer, F. P. G.; Kiani, A.; Edwards, J. P.; De Luna, P.; Bushuyev, O. S.; Zou, C. Q.; Quintero-Bermudez, R.; Pang, Y. J.; Sinton, D.; Sargent, E. H. CO_2 electroreduction to ethylene via hydroxide-mediated copper catalysis at an abrupt interface. *Science* **2018**, *360* (6390), 783−787.
(5) Li, F.; Thevenon, A.; Rosas-Hernandez, A.; Wang, Z.; Li, Y.; Gabardo, C. M.; Ozden, A.; Dinh, C. T.; Li, J.; Wang, Y.; Edwards, J. P.; Xu, Y.; McCallum, C.; Tao, L.; Liang, Z. Q.; Luo, M.; Wang, X.; Li, H.; O'Brien, C. P.; Tan, C. S.; Nam, D. H.; Quintero-Bermudez, R.; Zhuang, T. T.; Li, Y. C.; Han, Z.; Britt, R. D.; Sinton, D.; Agapie, T.; Peters, J. C.; Sargent, E. H. Molecular tuning of CO_2-to-ethylene conversion. *Nature* **2020**, *577* (7791), 509−513.
(6) Wang, Y.; Shen, H.; Livi, K. J. T.; Raciti, D.; Zong, H.; Gregg, J.; Onadeko, M.; Wan, Y.; Watson, A.; Wang, C. Copper Nanocubes for CO_2 Reduction in Gas Diffusion Electrodes. *Nano Lett.* **2019**, *19* (12), 8461−8468.
(7) Garcia de Arquer, F. P.; Dinh, C. T.; Ozden, A.; Wicks, J.; McCallum, C.; Kirmani, A. R.; Nam, D. H.; Gabardo, C.; Seifitokaldani, A.; Wang, X.; Li, Y. C.; Li, F.; Edwards, J.; Richter, L. J.; Thorpe, S. J.; Sinton, D.; Sargent, E. H. CO_2 electrolysis to multicarbon products at activities greater than 1 A cm^{-2}. *Science* **2020**, *367* (6478), 661−666.
(8) Verma, S.; Lu, S.; Kenis, P. J. A. Co-electrolysis of CO_2 and glycerol as a pathway to carbon chemicals with improved technoeconomics due to low electricity consumption. *Nature Energy* **2019**, *4* (6), 466−474.
(9) Gabardo, C. M.; O'Brien, C. P.; Edwards, J. P.; McCallum, C.; Xu, Y.; Dinh, C. T.; Li, J.; Sargent, E. H.; Sinton, D. Continuous Carbon Dioxide Electroreduction to Concentrated Multi-carbon Products Using a Membrane Electrode Assembly. *Joule* **2019**, *3* (11), 2777−2791.
(10) Choi, S.; Balamurugan, M.; Lee, K. G.; Cho, K. H.; Park, S.; Seo, H.; Nam, K. T. Mechanistic Investigation of Biomass Oxidation Using Nickel Oxide Nanoparticles in a CO_2-Saturated Electrolyte for Paired Electrolysis. *J. Phys. Chem. Lett.* **2020**, *11* (8), 2941−2948.
(11) Wang, Y.; Gonell, S.; Mathiyazhagan, U. R.; Liu, Y. M.; Wang, D. G.; Miller, A. J. M.; Meyer, T. J. Simultaneous Electrosynthesis of Syngas and an Aldehyde from CO_2 and an Alcohol by Molecular Electrocatalysis. *Acs Applied Energy Materials* **2019**, *2* (1), 97−101.
(12) Wang, D.; Wang, P.; Wang, S.; Chen, Y. H.; Zhang, H.; Lei, A. Direct electrochemical oxidation of alcohols with hydrogen evolution in continuous-flow reactor. *Nat. Commun.* **2019**, *10* (1), 2796.
(13) Perez-Gallent, E.; Turk, S.; Latsuzbaia, R.; Bhardwaj, R.; Anastasopol, A.; Sastre-Calabuig, F.; Garcia, A. C.; Giling, E.; Goetheer, E. Electroreduction of CO_2 to CO Paired with 1,2-Propanediol Oxidation to Lactic Acid. Toward an Economically Feasible System. *Ind. Eng. Chem. Res.* **2019**, *58* (16), 6195−6202.
(14) Sherbo, R. S.; Delima, R. S.; Chiykowski, V. A.; MacLeod, B. P.; Berlinguette, C. P. Complete electron economy by pairing electrolysis with hydrogenation. *Nature Catalysis* **2018**, *1* (7), 501−507.
(15) Li, T. F.; Cao, Y.; He, J. F.; Berlinguette, C. P. Electrolytic CO_2 Reduction in Tandem with Oxidative Organic Chemistry. *ACS Cent. Sci.* **2017**, *3* (7), 778−783.
(16) Wang, J. M.; Kong, R. M.; Asiri, A. M.; Sun, X. P. Replacing Oxygen Evolution with Hydrazine Oxidation at the Anode for Energy-Saving Electrolytic Hydrogen Production. *ChemElectroChem* **2017**, *4* (3), 481−484.
(17) Tang, C.; Zhang, R.; Lu, W. B.; Wang, Z.; Liu, D. N.; Hao, S.; Du, G.; Asiri, A. M.; Sun, X. P. Energy-Saving Electrolytic Hydrogen Generation: Ni2P Nanoarray as a High-Performance Non-Noble-Metal Electrocatalyst. *Angew. Chem., Int. Ed.* **2017**, *56* (3), 842−846.
(18) Hao, S.; Yang, L. B.; Liu, D. N.; Kong, R. M.; Du, G.; Asiri, A. M.; Yang, Y. C.; Sun, X. P. Integrating natural biomass electro-

oxidation and hydrogen evolution: using a porous Fe-doped CoP nanosheet array as a bifunctional catalyst. *Chem. Commun.* **2017**, *53* (42), 5710−5713.
(19) Na, J.; Seo, B.; Kim, J.; Lee, C. W.; Lee, H.; Hwang, Y. J.; Min, B. K.; Lee, D. K.; Oh, H. S.; Lee, U. General technoeconomic analysis for electrochemical coproduction coupling carbon dioxide reduction with organic oxidation. *Nat. Commun.* **2019**, *10* (1), 5193.
(20) Tuck, C. O.; Perez, E.; Horvath, I. T.; Sheldon, R. A.; Poliakoff, M. Valorization of Biomass: Deriving More Value from Waste. *Science* **2012**, *337* (6095), 695−699.
(21) Houache, M. S. E.; Safari, R.; Nwabara, U. O.; Rafaïdeen, T.; Botton, G. A.; Kenis, P. J. A.; Baranton, S.; Coutanceau, C.; Baranova, E. A. Selective Electrooxidation of Glycerol to Formic Acid over Carbon Supported $Ni_{1-x}M_x$ (M = Bi, Pd, and Au) Nanocatalysts and Coelectrolysis of CO_2. *ACS Applied Energy Materials* **2020**, *3* (9), 8725−8738.
(22) Houache, M. S. E.; Hughes, K.; Baranova, E. A. Study on catalyst selection for electrochemical valorization of glycerol. *Sustain Energ Fuels* **2019**, *3* (8), 1892−1915.
(23) Lucas, F. W. S.; Grim, R. G.; Tacey, S. A.; Downes, C. A.; Hasse, J.; Roman, A. M.; Farberow, C. A.; Schaidle, J. A.; Holewinski, A. Electrochemical Routes for the Valorization of Biomass-Derived Feedstocks: From Chemistry to Application. *Acs Energy Letters* **2021**, *6* (4), 1205−1270.
(24) Iglesias, J.; Martinez-Salazar, I.; Maireles-Torres, P.; Martin Alonso, D.; Mariscal, R.; Lopez Granados, M. Advances in catalytic routes for the production of carboxylic acids from biomass: a step forward for sustainable polymers. *Chem. Soc. Rev.* **2020**, *49*, 5704−5771.
(25) Smith, W. A.; Burdyny, T.; Vermaas, D. A.; Geerlings, H. Pathways to Industrial-Scale Fuel Out of Thin Air from CO_2 Electrolysis. *Joule* **2019**, *3* (8), 1822−1834.
(26) Li, T.; Harrington, D. A. An Overview of Glycerol Electrooxidation Mechanisms on Pt, Pd and Au. *ChemSusChem* **2021**, *14* (6), 1472−1495.
(27) Rabinowitz, J. A.; Kanan, M. W. The future of low-temperature carbon dioxide electrolysis depends on solving one basic problem. *Nat. Commun.* **2020**, *11* (1), 5231.
(28) Sisler, J.; Khan, S.; Ip, A. H.; Schreiber, M. W.; Jaffer, S. A.; Bobicki, E. R.; Dinh, C. T.; Sargent, E. H. Ethylene Electrosynthesis: A Comparative Techno-economic Analysis of Alkaline vs Membrane Electrode Assembly vs CO_2-CO-C_2H_4 Tandems. *Acs Energy Letters* **2021**, *6* (3), 997−1002.
(29) Jouny, M.; Hutchings, G. S.; Jiao, F. Carbon monoxide electroreduction as an emerging platform for carbon utilization. *Nature Catalysis* **2019**, *2* (12), 1062−1070.
(30) Ozden, A.; Wang, Y.; Li, F.; Luo, M.; Sisler, J.; Thevenon, A.; Rosas-Hernández, A.; Burdyny, T.; Lum, Y.; Yadegari, H.; Agapie, T.; Peters, J. C.; Sargent, E. H.; Sinton, D. Cascade CO_2 electroreduction enables efficient carbonate-free production of ethylene. *Joule* **2021**, *5* (3), 706−719.
(31) Salvatore, D.; Berlinguette, C. P. Voltage Matters When Reducing CO2 in an Electrochemical Flow Cell. *Acs Energy Letters* **2020**, *5* (1), 215−220.
(32) Zhang, Z.; Melo, L.; Jansonius, R. P.; Habibzadeh, F.; Grant, E. R.; Berlinguette, C. P. pH Matters When Reducing CO2 in an Electrochemical Flow Cell. *ACS Energy Letters* **2020**, *5*, 3101−3107.
(33) Ripatti, D. S.; Veltman, T. R.; Kanan, M. W. Carbon Monoxide Gas Diffusion Electrolysis that Produces Concentrated C_2 Products with High Single-Pass Conversion. *Joule* **2019**, *3* (1), 240−256.
(34) Martić, N.; Reller, C.; Macauley, C.; Löffler, M.; Reichert, A. M.; Reichbauer, T.; Vetter, K.-M.; Schmid, B.; McLaughlin, D.; Leidinger, P.; Reinisch, D.; Vogl, C.; Mayrhofer, K. J. J.; Katsounaros, I.; Schmid, G. $Ag_2Cu_2O_3$ - a catalyst template material for selective electroreduction of CO to C_{2+} products. *Energy Environ. Sci.* **2020**, *13* (9), 2993−3006.
(35) Weng, L. C.; Bell, A. T.; Weber, A. Z. Towards membrane-electrode assembly systems for CO_2 reduction: a modeling study. *Energy Environ. Sci.* **2019**, *12* (6), 1950−1968.
(36) Zhang, H.; Lin, X. R.; Chin, S.; Grinstaff, M. W. Synthesis and Characterization of Poly(glyceric Acid Carbonate): A Degradable Analogue of Poly(acrylic Acid). *J. Am. Chem. Soc.* **2015**, *137* (39), 12660−12666.
(37) Starr, J. N.; Westhoff, G. Lactic Acid. In *Ullmann's Encyclopedia of Industrial Chemistry*; Wiley-VCH, 2016.
(38) Dai, C. C.; Sun, L. B.; Liao, H. B.; Khezri, B.; Webster, R. D.; Fisher, A. C.; Xu, Z. C. J. Electrochemical production of lactic acid from glycerol oxidation catalyzed by AuPt nanoparticles. *J. Catal.* **2017**, *356*, 14−21.
(39) Zhou, Y. F.; Shen, Y.; Luo, X. L.; Liu, G.; Cao, Y. Boosting activity and selectivity of glycerol oxidation over platinum-palladium-silver electrocatalysts via surface engineering. *Nanoscale Advances* **2020**, *2* (8), 3423−3430.

https://doi.org/10.1021/acsenergylett.1c01639
ACS Energy Lett. 2021, 6, 3538−3544